Available online at www.sciencedirect.com
ScienceDirect
Trans. Nonferrous Met. Soc. China 24(2014) 2117−2121
Transactions of Nonferrous Metals Society of China
www.tnmsc.cn

Influence of sub-grain boundaries on quenching process of an Al−Zn−Mg−Cu alloy

Ke-da JIANG[1], Long CHEN[1], Yun-ya ZHANG[1], Yun-lai DENG[1,2]

1. School of Materials Science and Engineering, Central South University, Changsha 410083, China;
2. State Key Laboratory of High-performance Complex Manufacturing, Central South University, Changsha 410083, China

Received 17 October 2013; accepted 23 April 2014

Abstract: The effects of sub-grain boundaries on the quenching sensitivity and the precipitation behavior in Al−7.01Zn−1.26Mg−1.43Cu alloy were investigated by an end-quenching test. Specimens were solution treated at 440 °C and 480 °C to get different recrystallization fractions, respectively. The results show that the maximum hardness value of the Al−Zn−Mg−Cu alloy can be improved by the sub-grain boundaries, but the depth of age-hardening layer decreases significantly. The precipitation temperature and the activation energy are reduced by the changes of surface energy, which is induced by sub-grain boundaries. So, the precipitation process from η' phase to η phase becomes much easier. In this way, an increase in the number of sub-grain boundaries promotes the precipitation of $MgZn_2$ particles, especially η'-$MgZn_2$.

Key words: Al−Zn−Mg−Cu alloy; recrystallization; grain boundary; precipitation; quenching

1 Introduction

Al−Zn−Mg−Cu alloys are widely used in aviation and aerospace industries owing to their desirable strength, toughness and corrosion resistance [1]. The preparation method of Al−Zn−Mg−Cu alloy moves toward high strength, high toughness, and low quenching sensitivity, such as AA7085 and AA7081 [2,3]. The quenching sensitivity, which is especially critical for thick plats or heavy forgings of Al−Zn−Mg−Cu alloys, leads to inhomogeneity and drop of properties [4]. For its practical importance, many attempts have been made to understand the mechanisms responsible for quenching sensitivity and to reduce it [5,6]. So far, the researches about the quenching processes were mainly focused on the efficient control of the microstructure of Al−Zn−Mg−Cu alloys. Many studies have been conducted on the precipitation behavior of $MgZn_2$ [7,8] and on the efficient control of the microstructure [9,10] of Al−Zn−Mg−Cu alloys. Besides, the effects of compounds [11,12], quenching methods [13,14], and quenching medium [15] in quenching process have been studied and ascertained.

Generally, recrystallization should be prevented during the preparation of Al−Zn−Mg−Cu alloys because coarse recrystallized grains may deteriorate the strength, crack toughness, and stress corrosion resistance of the prepared alloys [16]. However, except dispersoid particles, many researches show that quenching sensitivity is also associated with sub-grain boundaries [16,17]. Unfortunately, less attention has been paid to the effect of sub-grain boundaries on the quenching process.

In the present study, specimens were solution treated at different temperatures to get different recrystallization fractions, respectively, and the effects of sub-grain boundaries on the quenching sensitivity and the precipitation behavior in an Al−Zn−Mg−Cu alloy during quenching were investigated by an end-quenching test.

2 Experimental

A thick plate with 118 mm in thickness was investigated. The composition of the experimental alloy was 7.04Zn, 1.26Mg, 1.43Cu, 0.07Zr (mass fraction, %)

Foundation item: Projects (2010CB731700, 2012CB619500) supported by the National Basic Research Program of China; Project (51375503) supported by the National Natural Science Foundation of China
Corresponding author: Yun-lai DENG; Tel: +86-731-88876931; E-mail: luckdeng@csu.edu.cn
DOI: 10.1016/S1003-6326(14)63321-5

with residual Al. Two bars with the dimensions of 40 mm×40 mm×118 mm were cut from the plate. The bars were fabricated as special specimens for an end-quenching test. After solution treated at 440 °C and 480 °C, respectively (noted as 440Q and 480Q), the specimens were quickly transferred to the end-quenching apparatus (less than 5 s), respectively, as shown in Fig. 1. The special specimen was griped vertically above a sprayer, which contacted a water pump. The sprayer sprayed water to the bottom of the specimen. The water gage was carefully controlled and the bottom of the specimen was fabricated a groove. In this way, the water would not be sprayed on the side of the specimen. At last, the quenched specimens were aged at 121 °C for 24 h.

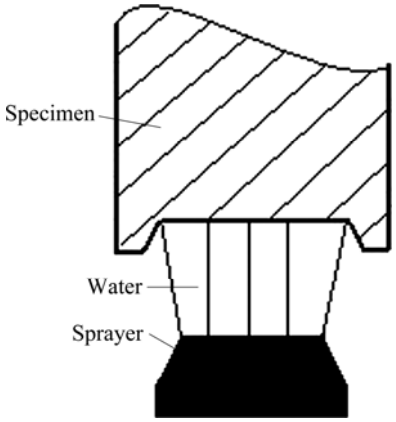

Fig. 1 Schematic diagram of the end-quenching apparatus

The specimens were studied by optical metallography (OM) using an XJP−6A microscope. A corrosive agent composed of 1 mL of HF, 16 mL of HNO_3, 3 g of CrO_3, and 83 mL of distilled water (Graff Sergeant agent) was used. The NET2SCH−200 F3 thermal analyzer was used for differential scanning calorimetry (DSC). Specimens were heated from room temperature to 475 °C with the heating rate of 5 °C/min. The Sirion 200 scanning electron microscope (SEM) was used to obtain the electron back scatter diffraction (EBSD) images. Experimental results of EBSD were analyzed by TSL OIM Analysis 5. The Vickers hardness tests were performed by applying 29.4 N load on the rolled surface of the specimen for 15 s.

3 Results and analysis

3.1 Inhomogeneity in microstructure and mechanical property

The OM images at different distances from the quenched surface of 440Q and 480Q samples are shown in Fig. 2. First of all, the specimen solution treated at higher temperature exhibited much higher recrystallization fraction. Specimens were etched by Graff Sergeant agent, which could etch $MgZn_2$ particles on grain and at sub-grain boundaries. Thus, grains filled with boundaries with low misorientation angles (<15°) appeared as a dark color, which could be identified as unrecrystallized ones. On the contrary, the grains of white color could be identified as recrystallized ones. Simply from the statistics of 10 OM images, the recrystallization fraction of 440Q sample was 23% and 480Q sample was 54%.

Moreover, we can find that the cooling rate had great influence on the precipitation of the second phase particles, which precipitated at grain boundaries and was etched easily. At the bottom of the specimens, on which water was sprayed directly, there were no visual second particles on the OM images. Both grain boundaries and grain areas are clear and we could not distinguish sub-grains from matrix. At the middle of the specimens, $MgZn_2$ particles were precipitated at sub-grain boundaries because of slower cooling rate, leading to a clear vision of sub-grain boundaries on the OM images. On the top of the specimens where had the slowest cooling rate, the dark color areas were darker. Besides, some second phase particles within grains can be seen in OM images. All phenomena expressed that these particles grew larger and precipitated more sufficient.

As shown in Fig. 3, the EBSD maps of the two specimens are highly identical with the OM images (Fig. 2). The 440Q sample basically kept the banded structure which formed during deformation (Fig. 3(a)). Within the elongated grains, there were a large amount of sub-grains. The 480Q sample, on the other hand, has some coarse recrystallized grains (Fig. 3(b)). These recrystallized grains were very clear, and there was no sub-grain boundary within them. Figure 3(c) shows a chart of grain boundary distributions of the two kinds of samples. It can be seen that the 440Q sample has much more grain boundaries under 15°.

Figure 4 shows the aging hardness and hardness retention values curves of the end-quenched samples. At the bottom of end-quenched specimens, the hardness was very high (Fig. 4(a)). This is because with high cooling rate, solid solubility is adequate, leading to better aging strengthening. The hardness became lower when the distance from bottom became larger, because course second phase particles precipitated during quenching may deteriorate the mechanical properties of alloys. It is apparent that the hardness of 440Q sample decreased faster than that of 480Q sample. In order to quantitatively describe effect of recrystallization on quenching sensitivity, the curves of hardness retention value vs depth are shown in Fig. 4(b). The hardness of 440Q sample decreased more than 10% while 480Q sample decreased around 5% from the bottom to the top of specimen. It can be known that, although the maximum hardness of 440Q sample is higher than 480Q

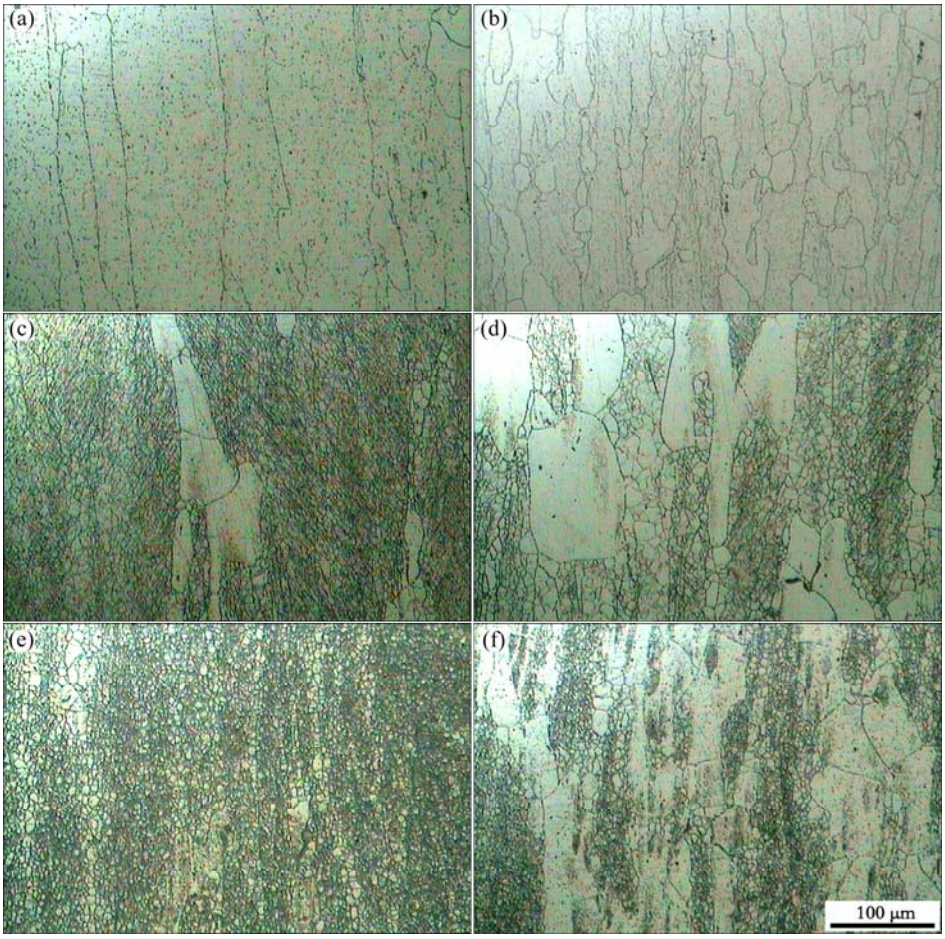

Fig. 2 OM images of different distances from quenched surface of 440Q and 480Q samples: (a) 440Q, surface; (b) 480Q, surface; (c) 440Q, 50 mm; (d) 480Q, 50 mm; (e) 440Q, 100 mm; (f) 480Q, 100 mm

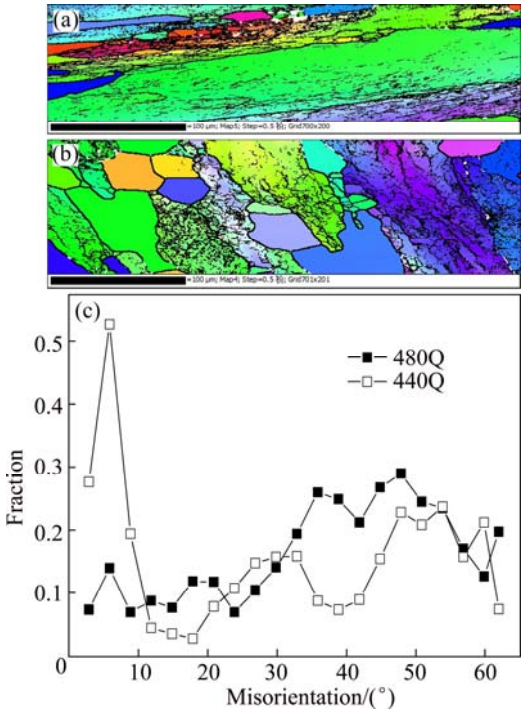

Fig. 3 EBSD maps of 440Q (a) and 480Q (b) specimens and grain boundaries distributions of two specimens (c)

sample (Fig. 4(a)), the hardening depths of the 480Q sample are apparently greater than the 440Q sample, as shown in Fig. 4(b). Thus, it suggests that the recrystallization can improve the hardenability.

3.2 Precipitation behavior

Figure 5 shows the DSC curves of 440Q and 480Q samples during cooling. Both the two curves exhibited two reactions, which were noted as I and II. Temperatures corresponding to the exothermic peaks in Fig. 5 are listed in Table 1. In line with former reports, exothermic reaction I represents the formation of η'-$MgZn_2$; exothermic reaction II represents the transformation of η'-$MgZn_2$ to η-$MgZn_2$. It can be seen that both η'-$MgZn_2$ and η-$MgZn_2$ precipitate earlier in 440Q sample than that in 480Q sample. Combined above results and discussion, we deem that the surface energy induced by sub-grain boundaries reduces the activation energy of precipitation of η'-$MgZn_2$ to η-$MgZn_2$, making η'-$MgZn_2$ to η-$MgZn_2$ precipitate more easily.

In general, the decomposition of supersaturated solid solution mainly depends on the fluctuations of

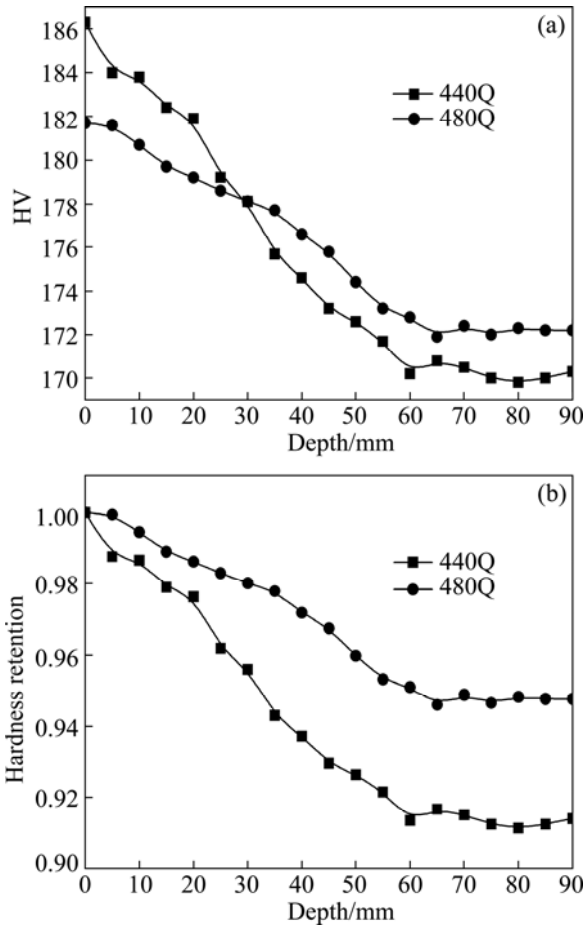

Fig. 4 Hardness curves of 440Q and 480 samples: (a) Vickers hardness; (b) Hardness retention

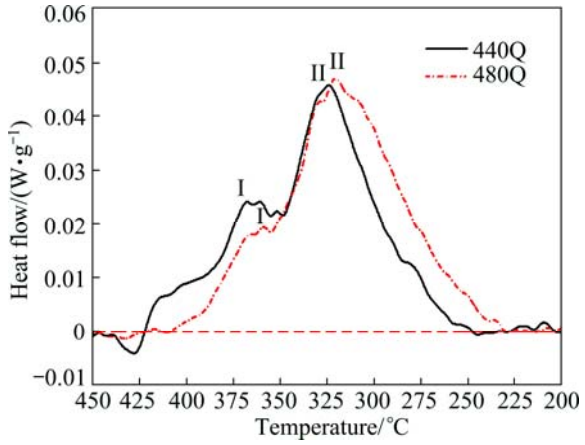

Fig. 5 DSC curves of 440Q and 480Q samples during cooling

Table 1 Temperatures corresponding to exothermic peaks in Fig. 5

Sample	Temperature/°C	
	I	II
440Q	368	324
480Q	359	322

energy and microstructure. The sub-grain boundary, which increases the microstructure fluctuations, is conducive to the nucleation. GP zones are considered to be of two types: GP I and GP II. GP I is an unstable phase and may dissolve into the matrix or directly transform to η'-$MgZn_2$ with an increase in the temperature [18]. On the contrary, GP II is relatively stable and may directly transform to η'-$MgZn_2$ or remain during heating [19]. The formation of both GP zones and η'-$MgZn_2$ phase needs a nucleation stage, but the transformation of η'-$MgZn_2$ to η-$MgZn_2$ is a type of allotropic transformation which has no nucleation stage. It can be inferred that the formation of GP zones and η'-$MgZn_2$ was severely affected by the sub-grain boundaries while η-$MgZn_2$ was mainly affected by the energy fluctuations offered by heating.

Figure 6 shows the TEM images and selected-area electron diffraction (SAED) patterns of the two kinds of samples (cut from the center) aged at 121 °C for 24 h. In the 440Q sample, a large number of sub-grain boundaries exist in the matrix. The η'-$MgZn_2$ particles preferentially nucleate and precipitate along the sub-grain boundaries, as shown in Fig. 6(a). In the 480Q sample, the volume fraction of sub-grain boundaries is very low, most of η'-$MgZn_2$ nucleated in grain relying on the energy

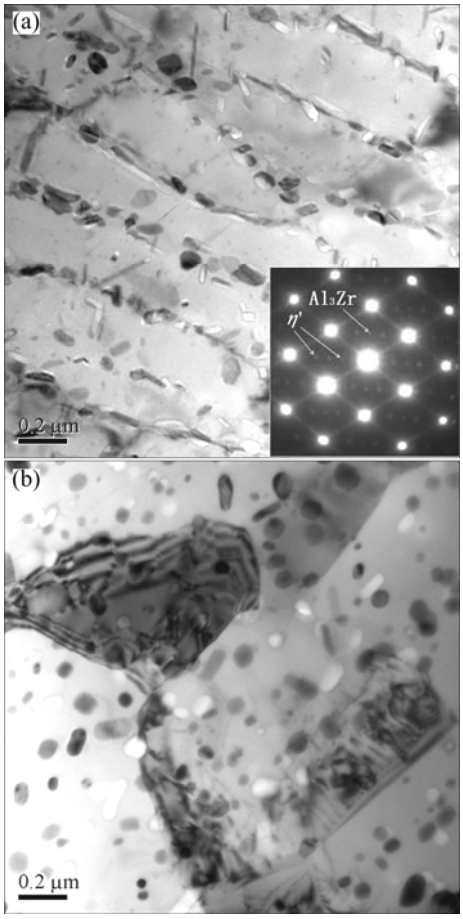

Fig. 6 TEM images of center samples in 440Q (a) and 480Q (b) aged at 121 °C for 24 h

fluctuations, as shown in Fig. 6(b). The observed microstructure corresponds to the above analysis.

4 Conclusions

1) The maximum hardness value of the Al−Zn−Mg−Cu alloy can be improved by the sub-grains, but the depth of age hardening layer decreases significantly.

2) As the sub-grain boundaries increases, the driving force of η'-$MgZn_2$ precipitation decreases, and the precipitation peak temperature rises.

3) With a large number of sub-grain boundaries, the η'-$MgZn_2$ particles preferentially nucleate and precipitate along the sub-grain boundaries. Conversely, most of η'-$MgZn_2$ nucleated in grain relying on the energy fluctuations in the recrystallized grains.

References

[1] WILLIAMS J C, STARKE J E. Progress in structural materials for aerospace systems [J]. Acta Materialia, 2003, 51(19): 5775−5799.

[2] LIU J. Advanced aluminum and hybrid aerostructures for future aircraft [J]. Materials Science Forum, 2006, 519: 1233−1238.

[3] CHAKRABARTI D J, LIU J, SAWTELL R R. New generation high strength high damage tolerance 7085 thick alloy product with low quench sensitivity [J]. Materials Forum, 2004, 28: 969−974.

[4] DESCHAMPS A, BRÉCHET Y. Characterization of precipitation microstructures in aluminum alloys 7040 and 7050 and their relationship to mechanical behavior [J]. Materials Science and Technology, 2004, 20(5): 567−576.

[5] LIM S T, YUN S J, NAM S W. Improved quench sensitivity in modified aluminum alloy 7175 for thick forging applications [J]. Materials Science and Engineering A, 2004, 371(1): 82−90.

[6] DESCHAMPS A, TEXIER G, RINGEVAL S, DELFAUT L. Influence of cooling rate on the precipitation microstructure in a medium strength Al−Zn−Mg alloy [J]. Materials Science and Engineering A, 2009, 501(1): 133−139.

[7] LIU S D, ZHANG X M, CHEN M A, YOU J H. Influence of aging on quench sensitivity effect of 7055 aluminum alloy [J]. Materials Characterization, 2008, 59(1): 53−60.

[8] DENG Y L, WAN L, ZHANG Y Y, ZHANG X M. Influence of Mg content on quench sensitivity of Al−Zn−Mg−Cu aluminum alloys [J]. Journal of Alloys and Compounds, 2011, 509(13): 4636−4642.

[9] LI P Y, XIONG B Q, ZHANG Y A, LI Z H, ZHU B H, WANG F, LIU H W. Quench sensitivity and microstructure character of high strength AA7050 [J]. Transactions of Nonferrous Metals Society of China, 2012, 22(2): 268−274.

[10] ZOU L, PAN Q L, HE Y B, WANG C Z, LIANG W J. Effect of minor Sc and Zr addition on microstructures and mechanical properties of Al−Zn−Mg−Cu alloys [J]. Transactions of Nonferrous Metals Society of China, 2007, 17(2): 340−345.

[11] HE Y D, ZHANG X M, YOU J H. Effect of minor Sc and Zr on microstructure and mechanical properties of Al−Zn−Mg−Cu alloy [J]. Transactions of Nonferrous Metals Society of China, 2006, 16(5): 1228−1235.

[12] LIU S D, ZHANG X M, CHEN M A. Effect of zirconium content on quench sensitivity of Al−Zn−Mg−Cu alloys [J]. Transactions of Nonferrous Metals Society of China, 2007, 17(4): 787−792.

[13] LIU S D, ZHANG Y, LIU W J, DENG Y L, ZHANG X M. Effect of step-quenching on microstructure of aluminum alloy 7055 [J]. Transactions of Nonferrous Metals Society of China, 2010, 20(1): 1−6.

[14] TANG J G, CHEN H, ZHANG X M, LIU S D, LIU W J, OUYANG H, LI H P. Influence of quench-induced precipitation on aging behavior of Al−Zn−Mg−Cu alloy [J]. Transactions of Nonferrous Metals Society of China, 2012, 22(6): 1255−1263.

[15] AMMAR H R, MOREAU C, SAMUEL A M, SAMUEL F H, DOTY H W. Influences of alloying elements, solution treatment time and quenching media on quality indices of 413-type Al–Si casting alloys [J]. Materials Science and Engineering A, 2008, 489(1): 426−438.

[16] SENKOV O N, SHAGIEV M R, SENKOVA S V, MIRACLE D B. Precipitation of Al_3(Sc, Zr) particles in an Al−Zn−Mg−Cu−Sc−Zr alloy during conventional solution heat treatment and its effect on tensile properties [J]. Acta Materialia, 2008, 56(15): 3723−3738.

[17] DENG Y L, ZHANG Y Y, WAN L, ZHANG X M. Effects of thermomechanical processing on production of Al−Zn−Mg−Cu alloy plate [J]. Materials Science and Engineering A, 2012, 554(1): 33−40.

[18] SHA G, CEREZO A. Early-stage precipitation in Al−Zn−Mg−Cu alloy (7050) [J]. Acta Materialia, 2004, 52(15): 4503−4516.

[19] JIANG X J, TAFTO J, NOBLE B, HOLME B, WATERLOO G. Differential scanning calorimetry and electron diffraction investigation on low-temperature aging in Al−Zn−Mg alloys [J]. Metallurgical and Materials Transactions A, 2004, 31(2): 339−348.

亚晶界对 Al−Zn−Mg−Cu 合金淬火过程的影响

姜柯达[1]，陈 龙[1]，张云崖[1]，邓运来[1,2]

1. 中南大学 材料科学与工程学院，长沙 410083；2. 中南大学 高性能复杂制造国家重点实验室，长沙 410083

摘 要：通过末端淬火试验研究了亚晶界对 Al−7.01Zn−1.26Mg−1.43Cu 合金淬火过程中的淬透性和第二相析出行为的影响。两组试样分别在 440 °C 和 480 °C 温度下固溶处理，以获得不同的再结晶分数。结果表明，亚晶界能够增大合金最大硬度值，但会明显降低淬透层深度。由于亚晶界的增加而引起的表面能的变化降低了相变激活能，故能够促进 η'相的形成及向 η 相的转变。

关键词：Al−Zn−Mg−Cu 合金；再结晶；晶界；析出相；淬火

(Edited by Hua YANG)